scientific reports

Check for updates

OPEN

Preparation of doped Mn, N-CDs and their application in the detection of ampicillin

Min Ye[1], Yinying Zhang[1], Pengpeng Ding[1] & Lifen Meng[1,2]✉

In this study, a one-step hydrothermal method was employed to synthesise highly fluorescent carbon quantum dots (Mn, N-CDs), incorporating the metallic element manganese (Mn) and the non-metallic element nitrogen (N). Banana peels and potassium permanganate were utilised as the raw materials. Characterisation methods were used to investigate the structure and properties of the Mn, N-CDs, revealing that they exhibited excellent fluorescence performance. The Mn, N-CDs was then applied as a fluorescent probe for penicillin detection, revealing that it significantly affected the fluorescence intensity of the Mn, N-CDs via a static quenching mechanism. Furthermore, the concentration of ampicillin sodium exhibited a strong linear relationship within the range of 0.05–20 μg/mL. Furthermore, antibiotics in environmental wastewater were analysed and spiked recovery experiments were performed. The results showed that ampicillin sodium recovery was 96.0-98.20%, with an RSD of less than 2.41%. In summary, this method provides a novel nanosensing platform for the rapid detection of antibiotic residues, with potential applications in environmental testing.

Keywords Biomass, Banana peel, Mn-nitrogen-codoped carbon dots, Fluorescent probe, Penicillin antibiotics

Antibiotics are drugs that are primarily used to treat bacterial infections. The first successful case of penicillin treatment in 1941 marked the beginning of its widespread use. The discovery of penicillin also led to rapid development in the pharmaceutical industry, with more than 160 new antibiotics or semisynthetic derivatives introduced by 1979[1–3]. However, the overuse of antibiotics in healthcare, animal husbandry and aquaculture means that many incompletely metabolised antibiotics enter the environment in their original form or as active ingredients through excreta[4]. These residues contaminate waterways via various pathways, leaving low concentrations of antibiotics in the environment over long periods. Prolonged exposure to these drugs may lead to bacteria gradually developing resistance, which could eventually result in the emergence of multidrug-resistant 'superbugs' and 'superviruses', posing a serious threat to human safety. In recent years, antibiotics have received widespread public attention, primarily due to the fact that drug abuse results in antimicrobial resistance and environmental pollution, and antibiotic residues have been found in almost all aquatic environments around the world. Therefore, new technologies or materials are needed worldwide to mitigate environmental pollution caused by improper wastewater treatment[6,7].

Although traditional analytical detection methods[8,9] can accurately analyse and detect antibiotics in the environment, their disadvantages-such as high time consumption, cost and technical requirements, limited selectivity and the inability to be used for on-site monitoring-limit their use. Therefore, the focus of current research is on highly selective and sensitive analytical detection methods that can be used efficiently for the detection of antibiotics in the environment.

Carbon dots (CDs) are a novel type of carbon nanomaterial with unique fluorescent properties. Like semiconductor nanomaterials, they are spherical or spherical-like particles that are usually less than 10 nm in size. Due to their superior properties, such as water solubility, photostability, biocompatibility and biotoxicity, they have received widespread attention in various applications[10,11]. In terms of analytical detection, the use of fluorescent carbon quantum dot probes has many advantages, including a fast response time, high sensitivity, simple equipment and ease of operation. This method is ideal for pollutant detection[12,13]. However, single-intensity-based fluorescent probe analysis methods are susceptible to interference from many factors independent of the analyte, such as variations in the local concentration of the probe, fluctuations in the excitation source, light scattering from the sample matrix and instrumental factors, such as the specific microenvironment around the probe[15,16]. Consequently, there has been growing interest in studying ratiometric fluorescent probes, where

[1]School of Chemical Engineering, Guizhou University of Engineering Science, Bijie, China. [2]Analytical & Testing Center, Guizhou University of Engineering Science, Bijie 551700, China. ✉email: 1025588702@qq.com

the analyte can differentially affect the emission peak intensity of dual-emission probes. Shortcomings of single-intensity fluorescence sensing methods can be overcome by establishing an internal reference ratio to provide a self-calibrated response signal, thereby increasing the accuracy of quantitative analysis[17–19]. Currently, many scholars have demonstrated that doping with heteroatoms can effectively enhance the optical properties of carbon quantum dots. Additionally, doping with metals increases the functional properties of carbon quantum dots[21–25].

In recent years, a great deal of research has been carried out by scholars on the preparation of carbon quantum dots and on analytical and detection methods for antibiotics in the environment. This research has focused on the following aspects, Deng et al.[25]synthesised antioxidant carbon dots (E-CDs) with excellent fluorescence properties using citric acid and ethylenediamine as raw materials. The quantum yield was 81.97%. The E-CDs exhibited a specific and sensitive response to •OH. The fluorescence of the E-CDs quenched by formed •OH could be restored through a competitive reaction with ampicillin (AMP). Roghayeh et al[26]. developed a ratiometric fluorescent sensor containing different coloured carbon dots (CDs) as dual fluorophores and a mesoporous, molecularly imprinted polymer receptor (B/YCDs@mMIP) for the detection of penicillin G (PNG) in milk.

In this study, the use of banana peel as a starting material for the synthesis of CDs is based on various considerations such as its rich chemical composition, environmentally friendly synthesis pathway, excellent product performance, and significant socio-economic benefits. This innovative method provides new ideas for the green synthesis of CDs and reflects the sustainable development concept of "turning waste into treasure".

The novelty and aim of the study were the use of banana peels as carbon source, potassium permanganate as source of manganese element to prepare Mn, N-CDs, which is environmentally friendly, cost-effective, non-toxic, and compared with traditional organic fluorescent molecules, the Mn, N-CDs has strong photostability and good resistance to photobleaching, solving the problem of signal attenuation in the detection of antibiotics in complex systems. The Mn, N-CDs provided an environmentally friendly, sensitive, stable, efficient and rapid analytical method for detecting penicillin antibiotics in the environment.

Experimental section

Reagents and instruments

Banana peels were purchased from supermarkets around the school. Erythromycin, roxithromycin, sulfamethoxypyridazine, clindamycin hydrochloride, clarithromycin and ampicillin sodium were purchased from Shanghai Myriad Chemical Science and Technology Co., Ltd.; potassium permanganate and potassium dihydrogen phosphate were purchased from Chengdu Kelong Chemical Reagent Factory; polyethylene glycol was purchased from Tianjin Guangfu Institute of Fine Chemical Industry; and hydrochloric acid was purchased from Zhejiang Longsheng Group, all of which were of analytically pure grade.Pulverizer (YB-800B, Yongkang Speed Front Industry & Trade Co., Ltd.), electronic balance (JA5003N, Shanghai Jinghai Instrument Co., Ltd.), vacuum drying oven (DZ-3BCII, Shanghai Aoanalytical Scientific Instrument Co., Ltd.), high-power numerical-control ultrasonic cleaner (KH-600KDE, Kunshan Wo Chuang Ultrasonic Instrument Co., Ltd.), electrothermal constant-temperature drum and air drying oven (DHG-9140 A, Shanghai Ranpai Industrial Co. 9140 A), Fluorescence spectrophotometer (F97PRO, Shanghai Prism Technology Co., Ltd.), Fourier transform infrared spectrometer (FTIR, WQF-530 A, Beijing Beifen Ruili Analytical Instruments), transmission electron microscope (TEM, JEOL JEM-F200, Japan), X-ray photoelectron spectrometer (XPS, Thermo Scientific K-Alpha, U.S.A.), desktop low-speed automatic balanced Centrifuge (TDZ4-WS, Changsha Meijiasen Instrument Co., Ltd.), Digital Magnetic Heating Jacket (CLT-1 A, Shanghai Li-Chen Bangxi Instrument Technology Co., Ltd.) were used in this experiment.

Preparation of Mn, N-CDs

Pretreatment of banana peels, rinsing, chopping, baking (220 °C, 1 h), Crushing into a fine powder. To prepare a polyethylene glycol aqueous solution with a concentration of 0.1 g/mL, 0.7 g of banana peel powder obtained from pretreatment was added to 70 mL of polyethylene glycol solution, 0.5 g of potassium permanganate was added, the mixture was stirred, the mixture was transferred to the reaction kettle and heated at 160 °C, the reaction was 7 h, and the kettle was removed and cooled at the end of the reaction. Then, the reaction mixture was filtered to remove solid particles by a 0.22 μm disposable filtration membrane and subsequently dialysed with 3000 Da dialysis bag for 48 h. The above solution transferred to a vacuum drying oven at 105 °C for 6 h. Finally, it was ground into powder with a mortar and pestle and stored in a sealed bag in a cool place.

Characterization of the Mn, N-CDs and fluorescence quantum yield determination

The fluorescence spectra of the Mn and N-CDs and their intensities were obtained with a fluorescence spectrophotometer (FS) to determine the optimal emission and excitation wavelengths. UV analysis was carried out via an ultraviolet-visible (UV) absorption spectrometer. The morphology and particle size of the Mn and N-CDs were characterized via transmission electron microscopy (TEM), and the ratios of their elemental compositions were determined via X-ray photoelectron spectroscopy (XPS). The functional groups on the surface of the prepared Mn, N-CDs were identified by a FTIR spectrophotometer. Mixed Mn, N-CDs powder with KBr powder in a ratio of 1:100, then thoroughly grind and mix the sample evenly, and then load it into a compression mold and press it into shape. The resolution of the FTIR used for measuring samples is 4 cm^{-1}, and the sample is scanned 20 times with a scanning range of 400 cm^{-1} to 4000 cm^{-1}. The quantum yield (QY) of quinine sulfate, which dissolved in 0.1 M H_2SO_4, was specified as a reference. The QY value of quinine sulfate was determined as 54% under excited wavelength of 360 nm. Based on the equation, calculating the QY value of Mn, N-CDs was calculated, $Q_{CDs}=Q_R(I_{CDs}/I_R)(A_R/A_{CDs})(\eta^2_{CDs}/\eta^2_R)$.

Detection of antibiotics by Mn, N-CDs

Mix 1mL of different concentrations of ampicillin sodium solution (0–20 μg/mL), 50 μL of Mn, N-CDs (0.01 g/mL), and 2 mL of acetate buffer solution (pH 3.0) with distilled water to a volume of 5 mL. Mix with an ultrasonic cleaner for 30 min, then measure the fluorescence intensity at excitation wavelength of 451 nm and emission wavelength of 515 nm and record the data (F).

In order to detect the interference of Mn, N-CDs fluorescent probes on ampicillin in complex samples, 1 ml of antibiotic solutions with a concentration of 10 μg/mL (erythromycin, roxithromycin, sulfamethoxypyridazine, clindamycin hydrochloride, clarithromycin and ampicillin sodium) were measured, respectively. Then add 50 μL of Mn, N-CDs fluorescent probe solution and dilute the mixed solution to 5 mL with deionized water. Mix with an ultrasonic cleaner for 30 min, transfer the reacted solution to a quartz colorimetric dish, and measure the fluorescence intensity (F) using fluorescence spectrophotometry. Record the fluorescence intensity of blank Mn, N-CDs solution was F_0.

Conditioned reaction experiments

Mixed 1 ml of ampicillin sodium solution with 50 μL of CDs solution, then add 2 ml of acetate buffer solutions with 5 different pH values (pH 2, 3, 4, 5, and 6), and dilute to 5 ml with distilled water. The reaction was carried out in an ultrasonic cleaner for 45 min. Determined the optimal pH value for the antibiotic reaction by measuring the fluorescence intensity at excitation wavelength of 451 nm and emission wavelength of 515 nm.

A total of 5 groups of 1 mL ampicillin sodium solution, 50 μL carbon solution and 2 mL acetate buffer solution (pH 3) were mixed with distilled water, fixed to 5 mL, and reacted at five different sonication times (15 min, 30 min, 45 min, 60 min, and 75 min). The optimum sonication time for the antibiotic reaction was determined by measuring and recording the fluorescence intensity at an excitation wavelength of 451 nm and an emission wavelength of 515 nm via a fluorescence spectrophotometer.

Five different amounts of CDs (30 μL, 35 μL, 40 μL, 45 μL, 50 μL) were added to 1 mL of ampicillin sodium solution (pH 3, 2 mL acetate buffer solution), and the mixture was fixed to 5 mL of distilled water. The reaction was carried out in an ultrasonic cleaner for 45 min. With the help of a fluorescence spectrophotometer, the fluorescence intensity was measured at an excitation wavelength of 451 nm and an emission wavelength of 515 nm and recorded to obtain the optimum amount of carbon quantum dots for this antibiotic reaction.

Plotting of standard curves

The ampicillin sodium solution was diluted to 0.05, 5, 10, 15–20 μg/mL, and 1 mL of each of the above five different concentrations of the solution was added to a test tube. Under the same experiment (pH 3, 45 min, 40 μL of CDs), measured their fluorescence intensity and record the data, and draw a standard curve between concentration and fluorescence quenching efficiency to determine its linear relationship.

Testing of actual samples

Lake water in front of the school library was collected and centrifuged at 1000 rpm for 10 min. It was then filtered through a 0.22 μm filter to remove impurities. The prepared drug was then added to the lake water, and the concentration of the drug in the lake water was calculated and recorded. The reaction was performed under the optimal conditions determined above (pH, time, amount of carbon dots, etc.). Finally, the fluorescence intensity values were measured at the same wavelengths, recorded, and the concentrations of the drug and recovery were calculated.

Results and discussion

Characterization and analysis of the Mn, N-CDs

FT-IR analysis of the Mn, N-CDs

FT-IR allowed the identification of the presence of functional groups in the prepared samples. Figure 1 shown the FT-IR spectra of the Mn, N-CDs. The broad absorption band at 3600–3400 cm^{-1} was a characteristic peak formed by O-H and N-H. the absorption peaks at 3000–2800 cm^{-1} and 1110.15 cm^{-1} were attributed to -COOH.

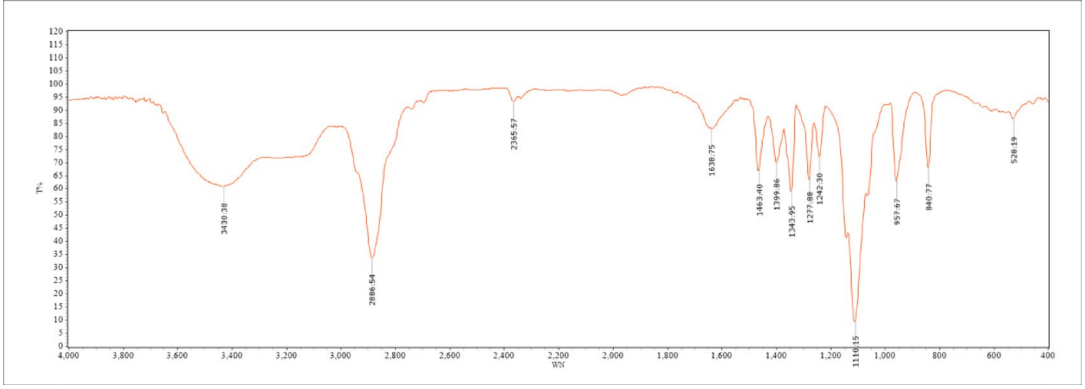

Fig. 1. Infrared spectra of Mn, N-CDs.

The absorption peak at 3500 ~ 3300 cm^{-1} corresponded to N-H, at 2886.54 cm^{-1} corresponded to -CH_3, at 1463.40 cm^{-1} corresponded to C-H, and at 528.19 cm^{-1} corresponded to Mn-O. The above results shown that the CDs contained hydrophilic oxidizing groups such as hydroxyl, carboxyl and amino groups and indicated that Mn and N atoms had been successfully doped into the CDs.

TEM analysis of the Mn, N-CDs

TEM was used to characterize the size and morphology of the Mn, N-CDs. Figure 2 shown electron micrographs of the samples at 200 nm, 1 μm and 10 μm, respectively, and the figures revealed that the prepared Mn, N-CDs were spherical with a relatively uniform particle size distribution, and agglomerations of these Mn, N-CDs were not observed, and the dispersion was relatively good. The average nanoparticle size was 5 nm.

XPS analysis of the Mn, N-CDs

From the Fig. 3(a), it could be seen that the XPS spectra of the Mn, N-CDs had four major characteristic peaks at 285.28, 537.38, 399.08, and 640.62 eV, which were C1s, O1s, N1s, and Mn2p, and the percentages were 67.59%, 30.11%, 1.2%, and 1.1%, respectively. The C1s were divided into three main peaks, 283.78 eV (C-C/C = C) and 285.18 eV (C = N/C-O) (Fig. 3b), the N1s also was divided into two main peaks, 398.03 eV (Mn-N) and 399.70 eV (Graphitic-N) (Fig. 3c), and the O1s was divided into three main peaks, 530.08 eV (Mn-O), 531.57 eV (-OH) and 531.98 eV (C = O) (Fig. 3d). The Mn2p peak at 640.62 eV was attributed to Mn-O. The above XPS analysis revealed that Mn and N atoms were successfully doped into the CDs. The appearance of these peaks indicated that the Mn, N-CDs were dominated by carbocyclic rings and contained abundant water-soluble functional groups, which was similar to the characterization results of FT-IR.

Spectral properties of Mn, N-CDs

The optical properties of the Mn, N-CDs were investigated using fluorescence (FS) and ultraviolet–visible (UV–vis) absorption spectroscopy. As illustrated in Fig. 4(b), a characteristic absorption peak was observed at 281 nm, resulting from the π–π* electron transition of the aromatic sp^2 carbon in the Mn, N-CDs. Figure 4(a) shows that the optimum excitation wavelength for the Mn, N-CDs was 450 nm and the optimum emission wavelength was 515 nm. The inset in Fig. 4(b) shows that the Mn, N-CDs solution appeared yellowish under sunlight and blue under a 365 nm UV lamp. The fluorescence quantum yield of the Mn, N-CDs was found to be 22.25%, using quinine sulfate as a reference.

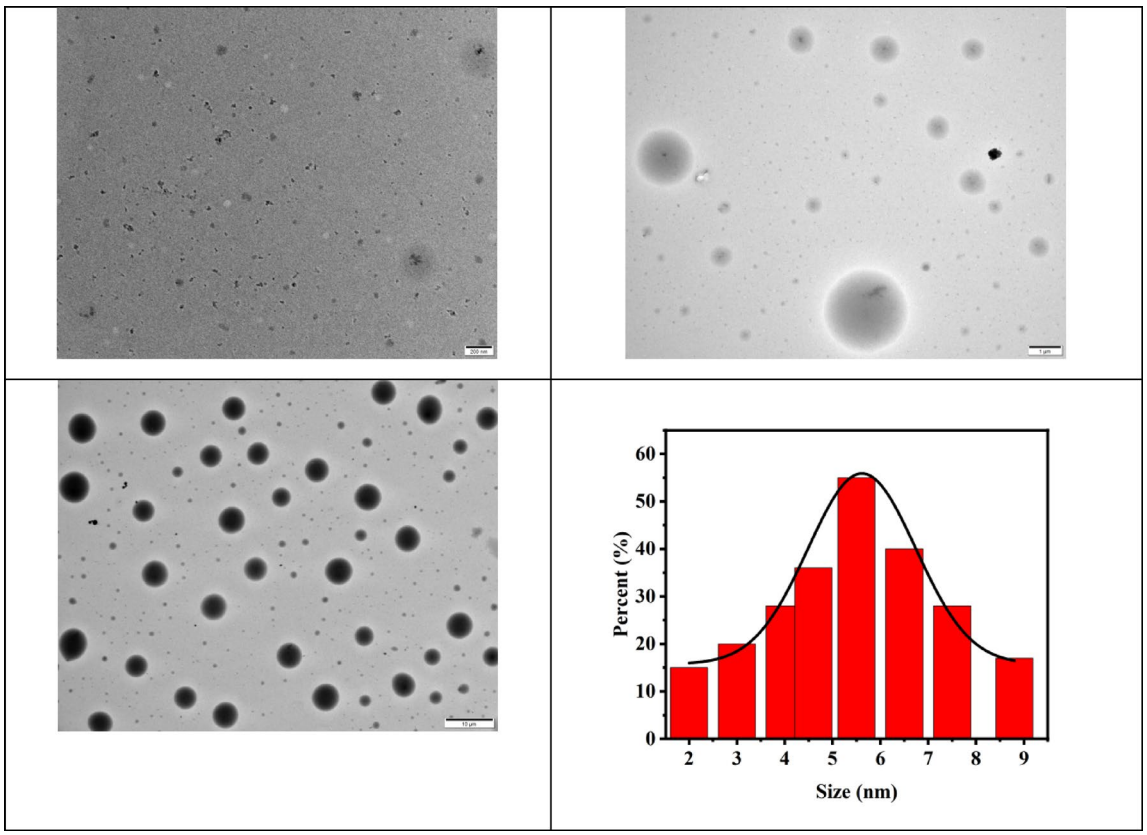

Fig. 2. TEM spectra of Mn, N-CDs at 200 nm, 1 μm and 10 μm, respectively. The below illustration: the filter diameter distribution map of the Mn, N-CDs.

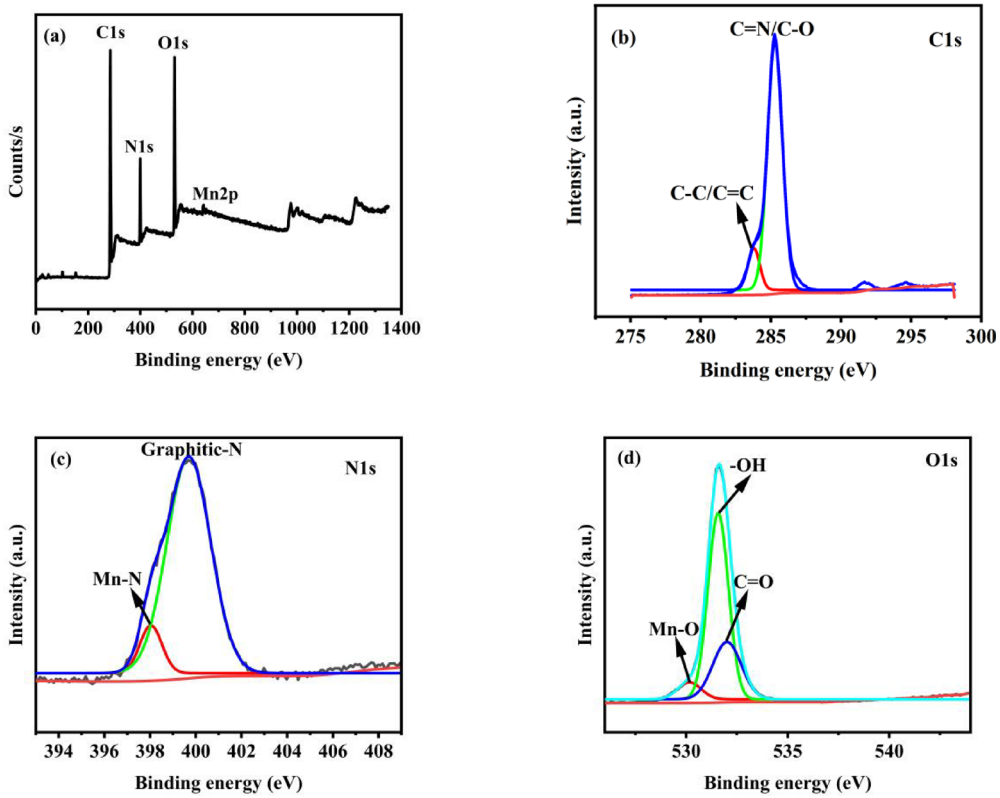

Fig. 3. (**a**) XPS survey scan, (**b**) C1s XPS, (**c**) N1s XPS, (**d**) O1s XPS of Mn, N-CDs.

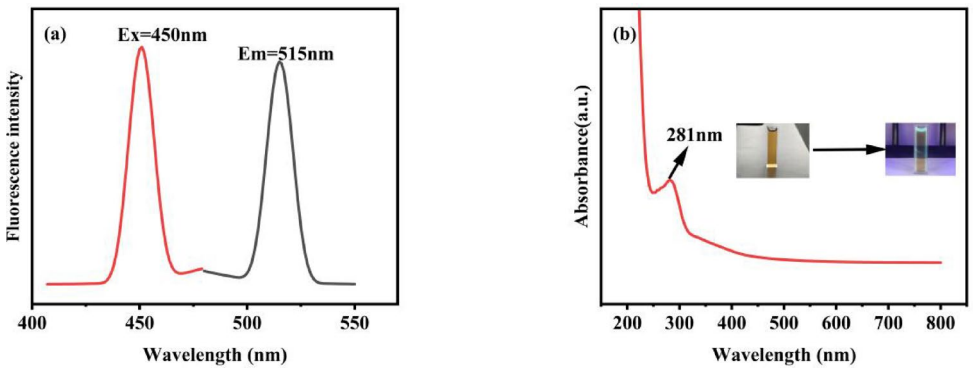

Fig. 4. (**a**) Excitation (red line), emission (black line) and (**b**) UV-visible absorption spectra of Mn, N-CDs. Illustration: A photograph of Mn, N-CDs in visible light (left) and ultraviolet light (right).

The stability of Mn, N-CDs

To verify the stability of the Mn, N-CDs, the change in the fluorescence intensity of the Mn, N-CDs was measured after being stored at 4 °C for one month. As shown in Fig. 5(a), the fluorescence intensity remained stable without significant changes. This indicated that the Mn, N-CDs had strong photostability.

Under illumination, the fluorescence intensity of the Mn, N-CDs changes with time, as shown in Fig. 5(b). The decreasing trend of fluorescence intensity of Mn, N-CDs with time is more obvious within 0 ~ 72 min. Within 72 ~ 240 min, the decreasing trend of fluorescence intensity becomes slower, indicating that Mn, N-CDs have excellent photostability.

Acetate buffer solutions with pH values ranging from 2.0 to 12.0 were added to the Mn, N-CDs in sequence. The experimental results are shown in Fig. 5(c). When the pH of the acetate buffer solution was between 2 ~ 6, the fluorescence quenching efficiency was relatively stable, significantly decreased at pH 7, which might be the transition of surface functional group protonation state, reversal of surface charge state, mutation of aggregation behavior, and changes in the competitive relationship between radiation/non radiation composite pathways and

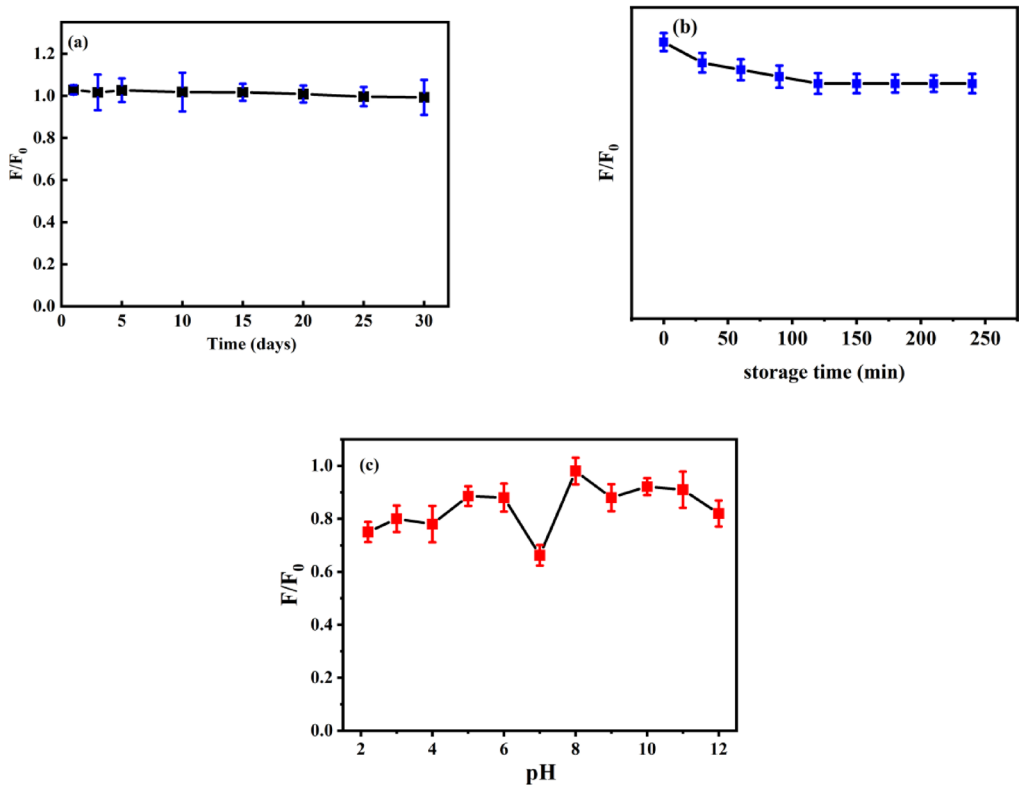

Fig. 5. (**a**) Effect of different storage time, (**b**) The influence of illumination time, and (**c**) pH on fluorescence efficiency of Mn, N-CDs.

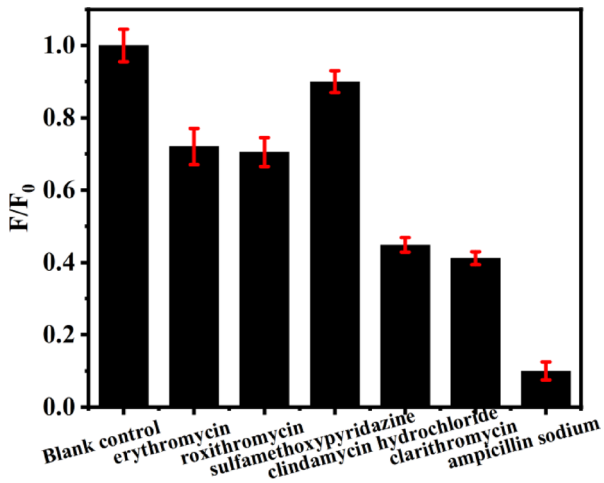

Fig. 6. Effect of different antibiotics on fluorescence intensity of Mn, N-CDs ($n = 3$).

slightly decreased but not very significantly above pH 8. This indicated that the Mn, N-CDs could be used as fluorescent nanoprobes in acidic and alkaline media.

Selectivity of Mn, N-CDs

The changes in fluorescence intensity were obtained via the reactions of six different antibiotics with the prepared Mn, N-CDs in neutral, acidic and basic buffer solutions. From the analysis of the data in Fig. 6, it can be concluded that the effects of the Mn, N-CDs on ampicillin were significant, whereas the effects on the other five antibiotics were not obvious. As shown in Fig. 6, ampicillin sodium had the best fluorescence quenching efficiency under acidic conditions.

Optimization of detection conditions

To improve the performance of the Mn, N-CDs for the detection of ampicillin sodium, several variables affecting the detection were specifically optimized, including the pH, response time and amounts of Mn, N-CDs. The quenching efficiency was F/F_0 throughout the experiment, where F and F_0 are the fluorescence intensities of the Mn, N-CDs with and without the addition of sodium ampicillin, respectively. When the pH was varied between 2.0 and 6.0 with the acetate buffer solution, there was a significant change in the fluorescence quenching efficiency of the solution, and the optimized value was pH 3, as shown in Fig. 7 (a). Similarly, the response time and amount of Mn, N-CDs were optimized to 45 min and 40 µL, as shown in Fig. 7 (b) and (c), respectively.

Linearity and selectivity

To verify the sensitivity of the method. Under the optimal conditions (pH 3, 45 min, 40 µL), different fluorescence intensities were obtained by adding different concentrations of ampicillin sodium, the data were recorded, and a standard curve was plotted, as shown in Fig. 8. When the concentration of ampicillin sodium was in the range of 0.05 ~ 20 µg/mL, the F/F_0 and the concentration of ampicillin sodium had a good linear relationship with an equation of $F/F_0 = 0.19311 + 0.03723$ C, R^2 was 0.99882, and the LOD for ampicillin sodium was calculated as 0.038 µg/mL on the basis of 3σ/S (where S represents the slope of the first fitting equation, σ is the standard deviation of the blank solution, and $n = 10$). Therefore, the prepared Mn, N-CDs as fluorescent probes had high sensitivity to ampicillin sodium and good potential for use in environmental detection.

Detection of actual samples

Different concentrations of ampicillin sodium (1 µg/mL, 5 µg/mL and 10 µg/mL) and Mn, N-CDs were added to the treated lake water for the reaction under the optimal experimental conditions. As shown in Table 1, the spiked recoveries of ampicillin sodium at different concentrations were 96.0%, 98.20% and 97.40%, with RSDs of 1.38%, 2.41%, and 1.40%, respectively. Therefore, the Mn, N-CDs produced from banana peels as carbon sources and potassium permanganate as the doped metal element Mn have great potential for use as novel fluorescent probes for the detection of penicillin antibiotics in environmental water samples.

To confirm that this method presented an advance in the state of the art, a comparison with other sensors is shown in Table 2. The fluorescent probe synthesis in this study exhibits unique characteristics in terms of high sensitivity, simple operation, and wide linear detection range compared to other reported fluorescent probes.

Mechanisms of ampicillin sodium detection by Mn, N-CDs

According to the literature, the current quenching mechanisms of CDs included dynamic quenching, static quenching and internal filtration effects[32–35]. Dynamic quenching was mainly caused by collisions between the

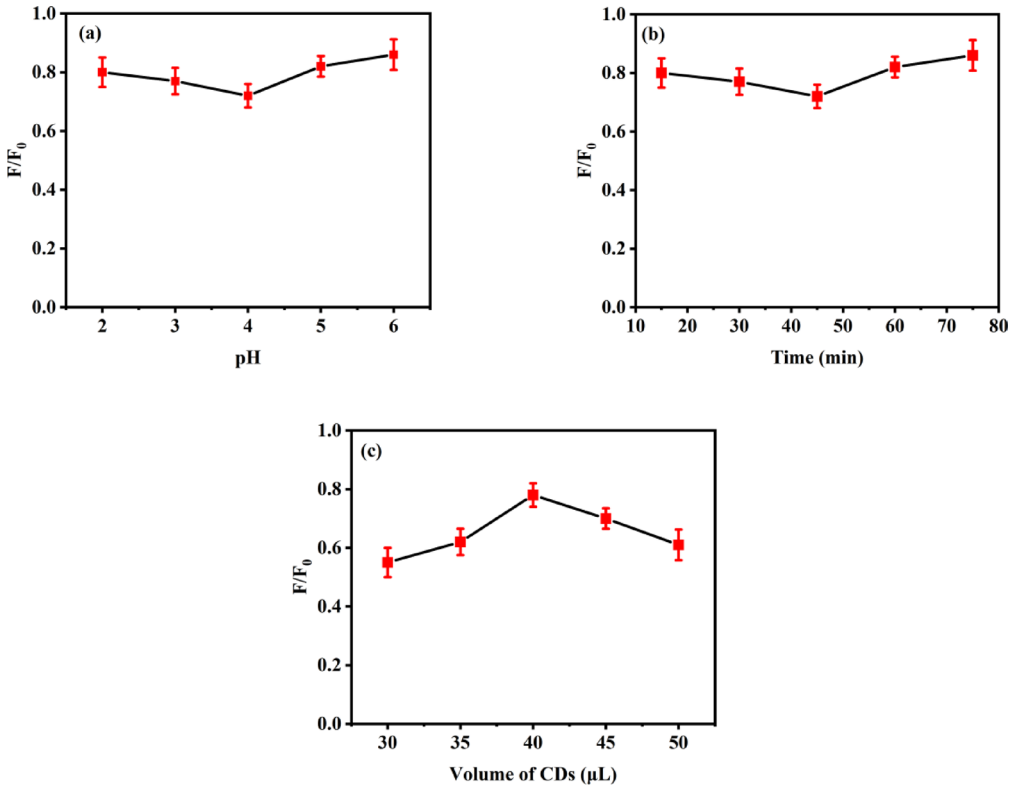

Fig. 7. (**a**) fluorescence quenching efficiency of Mn, N-CDs at different pH values, (**b**) Effects of different reaction time on the fluorescence quenching efficiency of Mn, N-CDs, (**c**) Effect of different amounts of Mn, N-CDs on fluorescence quenching efficiency ($n = 3$).

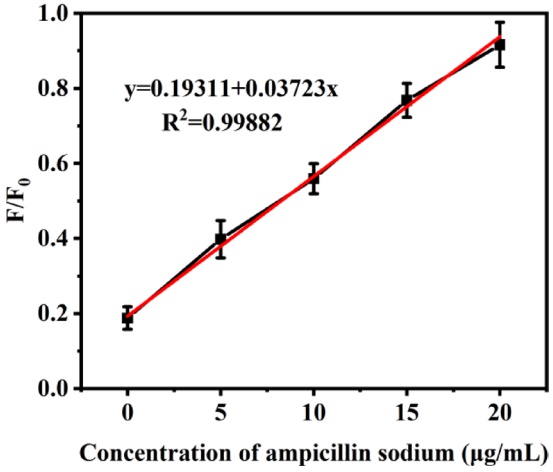

Fig. 8. The linear fitting plot of the fluorescence intensity of Mn, N-CDs and ampicillin sodium ($n = 3$).

Actual water samples	Spiked concentration (μg/mL)	Test concentration (μg/mL)	Spiked Recovery Rate (%)	RSD (%)
	1	0.96	96.0	1.38
Lake water	5	4.91	98.20	2.41
	10	9.74	97.40	1.40

Table 1. Preparation of Mn, N-CDs as fluorescent probes for the detection of ampicillin sodium in real water samples. ($n = 3$).

Sensors	Detecting antibiotics	LODs	Linear ranges	Samples	References
CdS QDs	Tetracycline	23nM	10 ~ 100μM	Water	[27]
$CsPbBr_3$ QDs/Boron Nitride	Tetracycline	6.5 mg/L	0 ~ 0.44 mg/L	Honey and milk	[28]
N-CQD@Co_3O_4	Nitrofurantoin	0.044μM	0.05–1220μM	Urine	[29]
RCQDs + BCQDs	Amoxicillin	2.39 nM	0–6 μM	lake water, eggs, and milk	[30]
B/YCDs@mMIPs	Penicillin-G	0.34 nM	1–32 nM	Milk	[26]
Mn, N-CDs	ampicillin sodium	0.038 μg/mL	0.05 ~ 20 μg/mL	Lake water	This work

Table 2. Comparison with reported methods for determination antibiotic. ($n = 3$).

luminescent material and the quencher, and the fluorescence lifetime changed significantly with or without the use of quencher[36,37]. Static quenching was mainly caused by the non-luminous or weakly fluorescent matrix complex formed by the interaction between the luminescent material and the quencher, and the fluorescence lifetime was basically unchanged with or without the quencher[38,39]. The internal filtration effect was a type of selective filtration phenomenon, which was essentially the process of re-absorption of light emitted by CDs[40–42].

Therefore, the UV-vis absorption spectra of the Mn, N-CD solutions before and after the addition of ampicillin sodium (1 mL, 10 μg/mL) were determined in this experiment. As shown in Fig. 9 (a), the UV-vis absorption spectra of the Mn, N-CD solutions red-shifted after the addition of sodium ampicillin, which could be attributed to π-π* jump, and the static quenching caused by the complexation of Mn, N-CDs and sodium ampicillin to produce nonluminous or weakly fluorescent ground state complex and the UV-visible absorption spectrum did not overlap with the fluorescence spectrum, indicating the absence of reabsorption effects. Meanwhile, the fluorescence lifetime curves before and after the addition of sodium ampicillin to Mn, N-CDs were also determined, and as shown in Fig. 9 (b), their fluorescence lifetimes remained essentially unchanged ($\tau_0 = 5.15137$ ns and $\tau = 5.13916$ ns, $\tau_0/\tau \approx 1$), which reinforced the mechanism of static quenching. The fluorescence quenching process of the Mn, N-CDs on antibiotics was shown in Fig. 10.

Conclusion

In this study, Mn N-CDs with excellent fluorescence properties were synthesised using a one-step hydrothermal method. Banana peels were employed as the biomaterial and potassium permanganate as the metal dopant. Characterisation of the Mn, N-CDs using FT-IR, TEM, and XPS showed that elemental Mn and N had been successfully doped into the Mn, N-CDs, which were found to be small in size with abundant surface functional

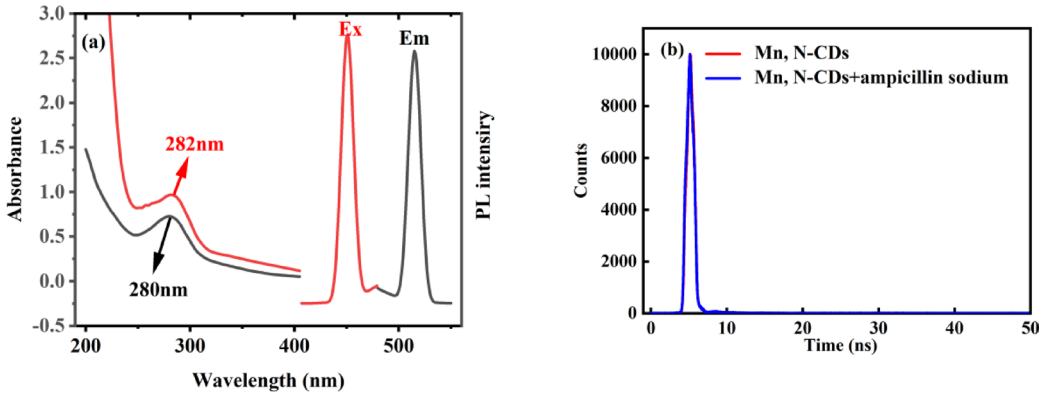

Fig. 9. (**a**) UV absorption spectra of Mn, N-CDs (black line) and ampicillin sodium + Mn, N-CDs (red line) and PL spectra of Mn, N-CDs, (**b**) Fluorescence lifetime decay curves of Mn, N-CDs and ampicillin sodium + Mn, N-CDs.

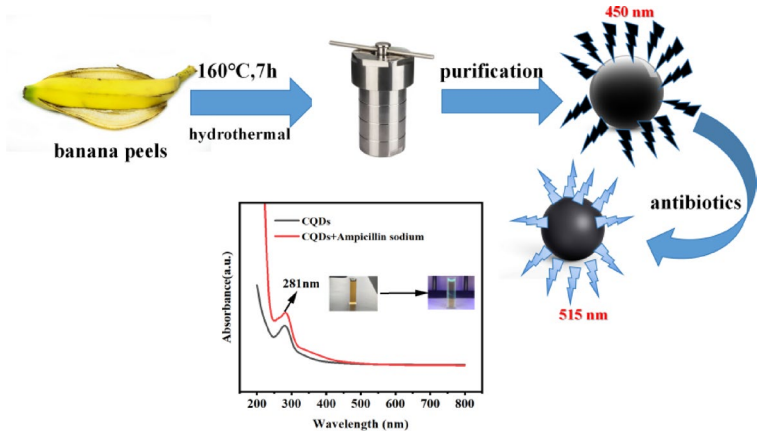

Fig. 10. Preparation of Mn, N-CDs and their application in antibiotic sensing research process.

groups and excellent fluorescence properties. The experiments concluded that adding sodium ampicillin significantly altered the fluorescence intensity of the Mn, N-CDs under acidic conditions. Spiking experiments on ampicillin sodium resulted in a small error (RSD < 5%) and high spiking recovery (88.60–93.20%). It can therefore be concluded that the prepared Mn, N-CDs are valuable for detecting antibiotics in the environment.

Data availability

All data generated or analysed during this study are included in this published article.

Received: 1 August 2025; Accepted: 1 October 2025
Published online: 06 November 2025

References

1. Thakare, R. et al. Antibiotics: past, present, and future. *Drug Discovery Target. Drug-Resistant Bacteria*, 1–8. (2020).
2. Watkinson, A. J. et al. The occurrence of antibiotics in an urban watershed: from wastewater to drinking water. *Sci. Total Environ.* **407** (8), 2711–2723 (2009).
3. Gholipour, S., Shamsizadeh, Z., Halabowski, D., Gwenzi, W. & Nikaeen, M. Combating antibiotic resistance using wastewater surveillance: Significance, applications, challenges, and future directions. *Sci. Total Environ.* **908** (1), 168056–168060 (2024).
4. Lu, N., Chen, J., Rao, Z., Guo, B. & Xu, Y. Recent advances of biosensors for detection of multiple antibiotics. *Biosens. (Basel).* **13** (9), 850–854 (2023).
4. Wei, L. et al. Aptamer-Based fluorescent DNA biosensor in antibiotics detection. *Food Res. Int.* **179** (1), 114005–114009 (2024).
5. Ding, Q. et al. β-Lactamase sensitive probe for rapid detection of antibiotic-resistant bacteria with gas chromatography-tandem mass spectrometry. *Anal. Chem.* **95** (14), 6098–6106 (2023).
6. Huang, Y. H. et al. Sensing antibiotics in wastewater using surface-enhanced Raman scattering. *Environ. Science&Technology*. **57** (12), 4880–4891 (2023).
7. Singh, H. et al. Nanomaterial-based fluorescent biosensors for the detection of antibiotics in foodstuffs: A review. *Food Chem.* **426** (1), 136657–136660 (2023).
8. Xu, X. Y. et al. Electrophoretic analysis and purification of fluorescent single-walled carbon nanotube fragments. *J. Am. Chem. Soc.* **126** (40), 12736–12737 (2004).

9. Das, R., Bandyopadhyay, R. & Pramanik, P. Carbon quantum Dots from natural resource:a review. *Mater. Today Chem.* **8**, 96–109 (2018).
10. Won, S. et al. Transformation of a cluster-based metal-organic framework to a rod metal-organic framewor. *Chem. Mater.* **34** (1), 273–278 (2022).
11. Wang, Y. et al. Ratiometric fluorescent paper sensor utilizing hybrid carbon Dots quantum Dots for the visual determination of copper ions. *Nanoscale* **8**, 5977–5984 (2016).
12. Cánchig, B. M. et al. Enhanced selectivity of carbon quantum Dots for metal ion detection through surface modification by heteroatom doping: a study on optical properties and theoretical approach. *Carbon Trends*. **18**, 100445–100445 (2025).
13. Huang, J. X. et al. An efficient metal-free phosphorus and oxygen codoped g-C_3N_4 photocatalyst with enhanced visible light photocatalytic activity for the degradation of fluoroquinolone antibiotics. *Chem. Eng. J.* **374**, 242–253 (2019).
14. Rahmah, S. A. et al. Structural characterization of carbon quantum Dots derived from tea residue and their photocatalytic application in CQDs-modified $Al_2(SO_4)_3$ nanoparticles for sustainable pesticide degradation. *Mater. Chem. Phys.* **334**, 130401–130401 (2025).
15. Kumar, S. H., Shamsudin, A. S. & Azian, A. N. M. Optimized nitrogen-doping of carbon quantum Dots from banana Peel waste: a highly selective Fe^{2+} sensor probe. *Diam. Relat. Mater.* **148**, 111351–111351 (2024).
16. Wang, J. et al. Bimetallic-doped carbon quantum Dots with enhanced photoluminescence and peroxidase-mimicking activity for dual-mode colorimetric and ratiometric fluorescence assay of alendronate. *Anal. Bioanal. Chem.*, **417**(15), 1–12. (2025).
17. Manikandan, V. & Lee, N. Y. Green synthesis of carbon quantum Dots and their environmental applications. *Environ. Res.* **212**, 113283 (2022).
18. Wang, Z. M. et al. Zinc-reduced carbon quantum Dots as color-conversion materials in blue light-emitting diodes. *ACS Appl. Nano Mater.* **7** (1), 940–950 (2024).
19. Yang, J. et al. One-step hydrothermal synthesis of near-infrared emission carbon quantum Dots as fluorescence aptamer sensor for cortisol sensing and imaging. *Talanta* **260**, 124607 (2023).
20. Wu, J. et al. Synthesis and applications of carbon quantum Dots derived from biomass waste: a review. *Environ. Chem. Lett.* **21** (6), 3393–3424 (2023).
21. Qandeel, N. A. et al. Fast one-pot microwave-assisted green synthesis of highly fluorescent plant-inspired S, N-self-doped carbon quantum Dots as a sensitive probe for the antiviral drug Nitazoxanide and hemoglobin. *Anal. Chim. Acta*. **1237**, 340592 (2023).
22. Nengtao Wu; Aiwen Yu; Lingbo Zhang. Wangqiang Liu; Jinwei Gao; Chengcheng Zhang; Yuhui Zheng. Biocompatible nanoplatform based on mussel adhesive chemistry: effective Assembly, dual mode Sensing, and cellular imaging performance. *Adv. Mater. Interfaces*. **6** (17), 1900732 (2019).
23. Qin Wen. Zhi Zeng; Wanqiang Liu; Jinwei Gao; Helen Meihua Zhang; Chengcheng Zhang; Yuhui Zheng. In vitro monitoring of glutathione via a switched-on effect based on a lanthanide incorporated carbon nanostructure with biocompatibility. *Synth. Met.* **257**, 116183 (2019).
24. Deng, X. et al. A facile fluorescence method for the effective detection of ampicillin using antioxidant carbon Dots with specific fluorescent response to ˙OH. *Analyst* **149**, 3651–3660 (2024).
25. Jalili, R. et al. Detection of penicillin G residues in milk based on dual-emission carbon Dots and molecularly imprinted polymers. *Food Chem.* **314**, 126172 (2020).
26. Narasimhappa, P., Singh, S. & Ramamurthy, P. C. Synthesis of water-soluble cds quantum Dots for the fluorescence detection of Tetracycline. *Environ. Pollut.* **338** (1), 122682–122686 (2023).
27. Wang, W., Deng, P., Liu, X., Ma, Y. & Yan, Y. A $CsPbBr_3$ quantum dots/ultra-thin BN fluorescence sensor for stability and highly sensitive detection of Tetracycline. *Microchem J.* **162**, 105876. https://doi.org/10.1016/j.microc.2020.105876 (2021c).
28. Muthusankar, G., Devi, R. K. & Gopu, G. Nitrogen-doped carbon quantum Dots embedded Co_3O_4 with multiwall carbon nanotubes: an efficient probe for the simultaneous determination of anticancer and antibiotic drugs. *Biosens. Bioelectron.* **150**, 111947 (2020).
29. Li, L. et al. Hydrogen-bond induced enhanced emission ratiometric fluorescent handy needle for visualization assay of amoxicillin by smartphone sensing platform. *J. Hazard. Mater.* **444(Pt A)**, Article130403. https://doi.org/10.1016/j.jhazmat.2022.130403 (2023).
30. Panigrahi, S. K. & Mishra, A. K. Inner filter effect in fluorescence spectroscopy: as a problem and as a solution. *J. Photochem. Photobiol., C*. **41**, 100318 (2019).
32. Lin, Q. et al. Dual-emission ratiometric fluorescence probe based on copper nanoclusters for the detection of Rutin and Picric acid. *Spectrochim. Acta Part A Mol. Biomol. Spectrosc.* **270**, 120829 (2022).
33. Elhaleem, A. M. S. et al. Quality by design-aided acid-free synthesis of self P, N, S-doped black seed-derived carbon quantum Dots for application as a nanosensor for Eltrombopag environmental and bioanalysis and Pharmacokinetic assay. *Spectrochim. Acta Part A Mol. Biomol. Spectrosc.* **319**, 124495 (2024).
34. Sh, M. S. E. A. Insights for applying N,S-doped carbon Dots as a fluorescent nanoprobe for Estimation of some nitro-calcium channel blockers. *Royal Soc. Open. Sci.* **9** (10), 220609 (2022).
35. M S E A, F E, H. S. S. et al. Utilization of N,S-Doped carbon Dots as a fluorescent nanosensor for determination of Cromolyn based on inner filter Effect; application to aqueous humor. *Luminescence:the J. Biol. Chem. Luminescence*. **37** (5), 713–721 (2022).
36. Elhaleem, A. M. S. et al. Lentils/urea as precursors for profound S and N doping of carbon Dots for selective sequential determination of Hg(II) and S(II) in food and environmental samples. *Microchem. J.* **201**, 110658 (2024).
37. Hadi, Z. et al. A DFT study on the therapeutic potential of carbon nanostructures as sensors and drug delivery carriers for Curcumin molecule:nbo and QTAIM analyses. *Colloids Surf. A:Physicochemical Eng. Aspects*. **651**, 129698 (2022).
38. Shymaa M Abd Elhaleem., et al. Turn-off fluorescence of nitrogen and sulfur carbon quantum Dots as effective fluorescent probes for determination of imatinib. Application to biological fluids. *Spectrochim. Acta A*. **272**, 120954–120954 (2022).
39. Pei, S. et al. Green Preparation of silanized carbon Dots with ficus virens leaves as a potent antibacterial agent and an effective fluorescent sensor of iron ion. *J. Lumin.* **260**, 119837 (2023).
40. Elhaleem, A. M. S. et al. Self-ratiometric fluorescence approach based on room-temperature instantaneously synthesized carbon Dots from folin's reagent and ethanolamine for determination of nitroxinil in water, milk, and food samples. *Anal. Chim. Acta*. **1323**, 343061 (2024).
41. Wu, X. et al. An optical and visual multi-mode sensing platform base on nitrogen, sulfur, Boron co-doped carbon Dots for rapid and simple determination of ferric ions in water. *Spectrochim. Acta Part A Mol. Biomol. Spectrosc.* **302**, 122995 (2023).
42. Elhaleem, A. M. S. et al. Room-temperature one-step instant synthesis of carbon Dots as a new sensing platform for the Estimation of hydroxocobalamin in water and food samples. *Microchem. J.* **208**, 112616 (2025).

Acknowledgements

This wok was financially supported by the Bijie City Science and Technology Bureau Joint Fund Project (2023[47] and 2023[46]), and the National Innovation and Entrepreneurship Project for College Students in 2024 of Guizhou University of Engineering Science (2024106680214 and 2024106680217).

Author contributions

Min Ye: Writing-original draft, Validation, Methodology, Data curation, Conceptualization. Yinying Zhang, Pengpeng Ding: Validation, Methodology. Methodology, Conceptualization. Lifen Meng: Writing-review & editing, Visualization, Supervision, Data curation, Conceptualization.

Declarations

Competing interests

The authors declare no competing interests.

Additional information

Correspondence and requests for materials should be addressed to L.M.

Reprints and permissions information is available at www.nature.com/reprints.

Publisher's note Springer Nature remains neutral with regard to jurisdictional claims in published maps and institutional affiliations.

Open Access This article is licensed under a Creative Commons Attribution-NonCommercial-NoDerivatives 4.0 International License, which permits any non-commercial use, sharing, distribution and reproduction in any medium or format, as long as you give appropriate credit to the original author(s) and the source, provide a link to the Creative Commons licence, and indicate if you modified the licensed material. You do not have permission under this licence to share adapted material derived from this article or parts of it. The images or other third party material in this article are included in the article's Creative Commons licence, unless indicated otherwise in a credit line to the material. If material is not included in the article's Creative Commons licence and your intended use is not permitted by statutory regulation or exceeds the permitted use, you will need to obtain permission directly from the copyright holder. To view a copy of this licence, visit http://creativecommons.org/licenses/by-nc-nd/4.0/.

© The Author(s) 2025